Supplementary Information for:
Advances in Geochemistry and Cosmochemistry 1(2): 986, https://doi.org/10.33063/agc.v1i2.986

Geochemical and isotopic (O-Fe-Sr-Nd) characterization of reference materials relevant to environmental impact assessments

Alex J. McCoy-West[1,2*], Dafne Koutamanis[1], Evelyne M. S. Leduc[3] and Brandon Mahan[4,1]

[1] IsoTropics Geochemistry Laboratory, Earth and Environmental Science, James Cook University, Townsville, Australia 4811

[2] Economic Geology Research Centre, James Cook University, Townsville, QLD, Australia

[3] Queen's Facility for Isotope Research, Department of Geological Sciences and Geological Engineering, Queen's University, Canada

[4] Melbourne Analytical Geochemistry, School of Geography, Earth and Atmospheric Sciences, University of Melbourne, Parkville, VIC 3010, Australia

*Corresponding author: alex.mccoywest@jcu.edu.au

Data, Code, and Outputs:

Geochemical dataset can be obtained from: https://doi.org/10.60520/IEDA/113997

1. Supplementary Figures

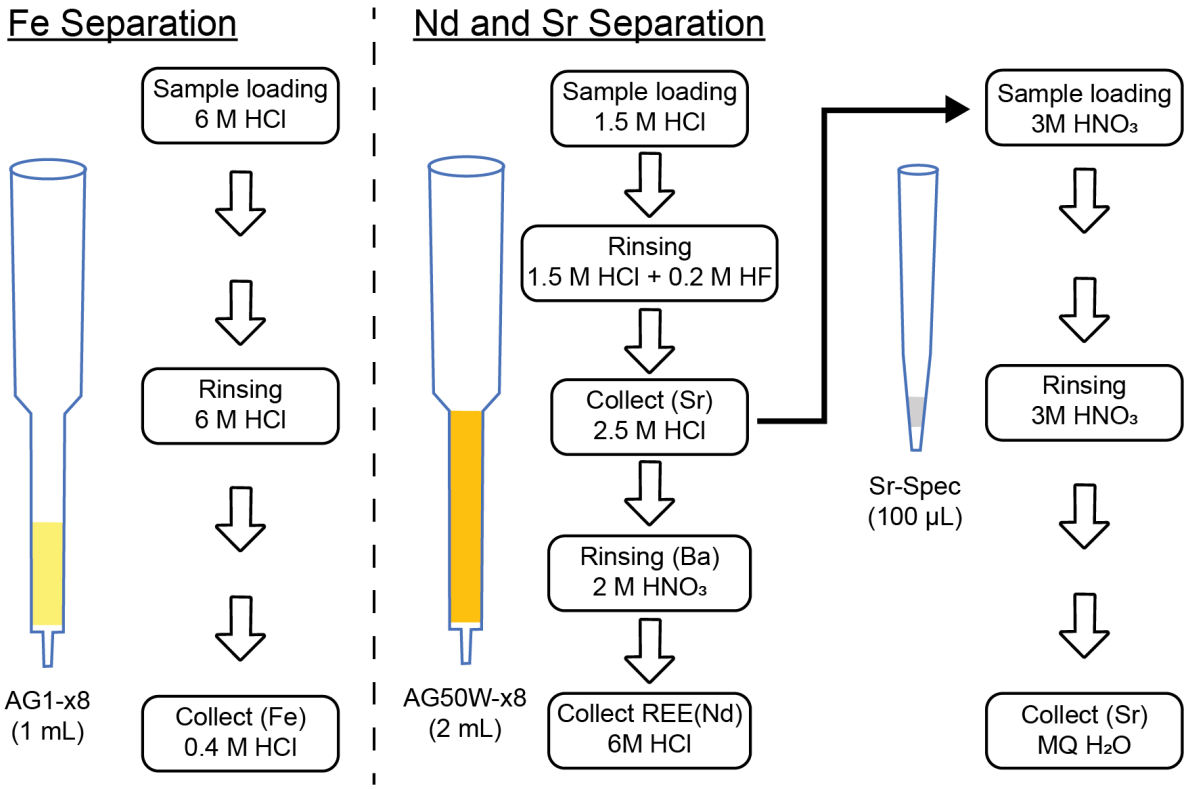

Figure S1: *Schematic diagram of the ion exchange chromatography procedure implemented prior to MC-ICP-MS analyses. Dotted line separates two independent chemical separation schemes.*

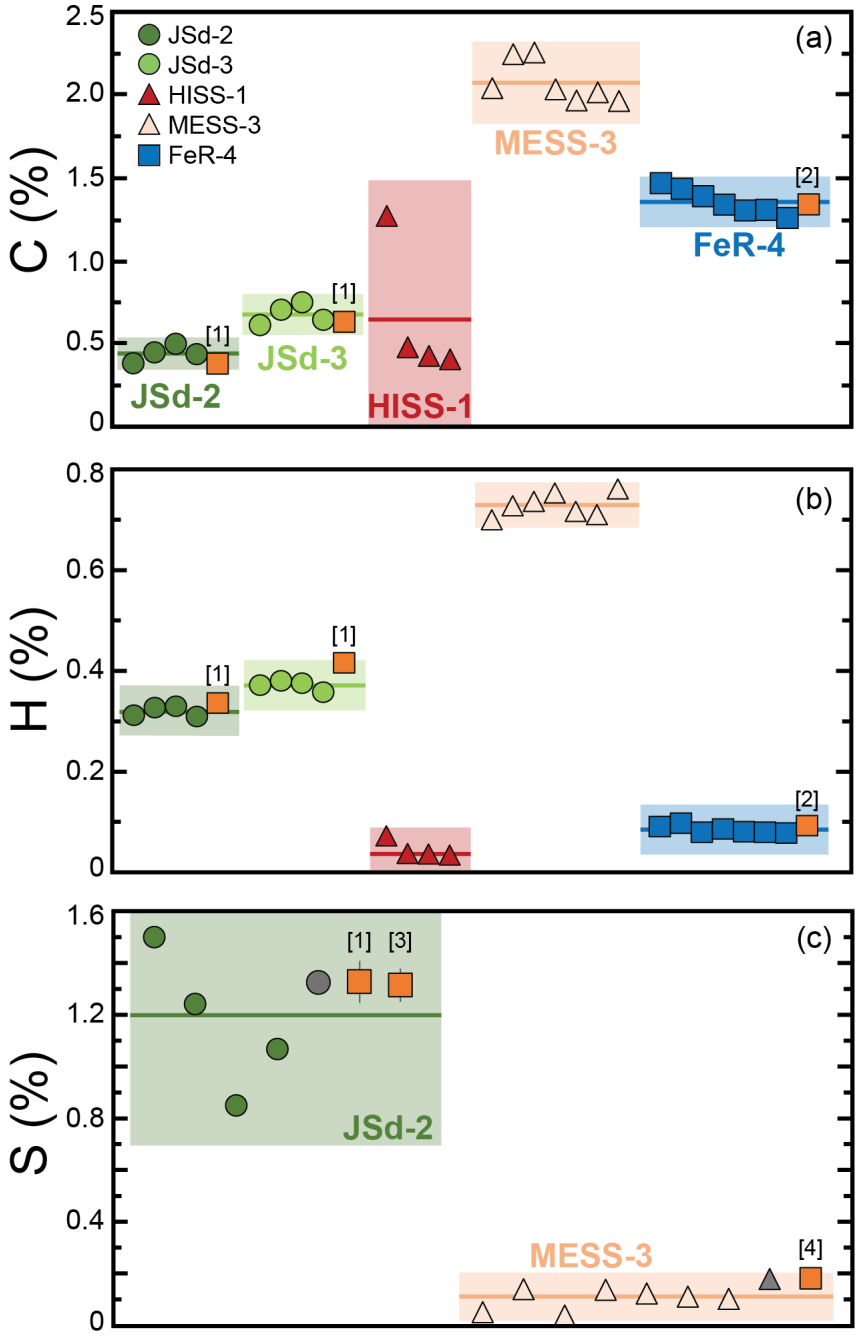

Figure S2: *Long-term repeatability of volatile element concentration measurements based on replicate analyses of RM. (a) Carbon; (b) Hydrogen; (c) Sulfur. Shaded fields represent average value (line) ± 2 standard deviations of population, except in (b) where it has been fixed at ± 0.05 % to be visible. Majority of analyses were undertaken using EA, except grey symbols in (c) which are from XRF measurements. Only RM that had measurable S contents in each duplicate are shown. Orange squares represent previously published values: [1] Kubota (2009); [2] Govindaraju (1994); [3] Imai et al. (1996); [4] average from GeoReM (Jochum et al., 2005). Note: some RM display significant intra aliquot heterogeneity.*

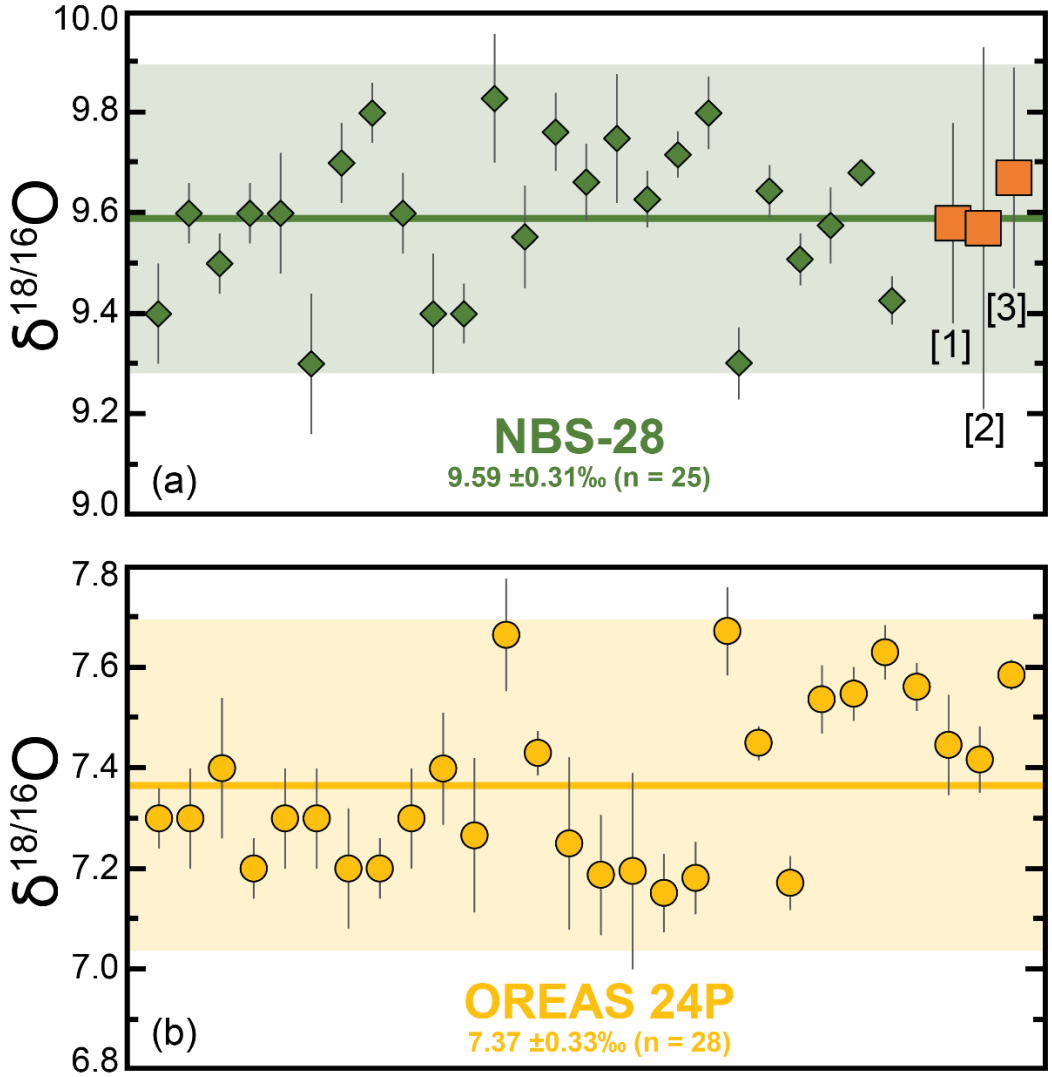

Figure S3: *Long-term repeatability of oxygen isotope measurements via IRMS in this study (a) Primary reference material NBS-28; (b) in-house basalt standard OREAS 24P. Uncertainty bars are measured 2 standard deviation values, with shaded fields representing average value (line) ± 2 standard deviations. Orange squares represent published $\delta^{18}O$ values 1) 9.58 ± 0.20 ‰ (Reed, 1992); 2) 9.57 ± 0.36 ‰ (Baker et al., 2000); 2) 9.67 ± 0.22 ‰ (Hou et al., 2003).*

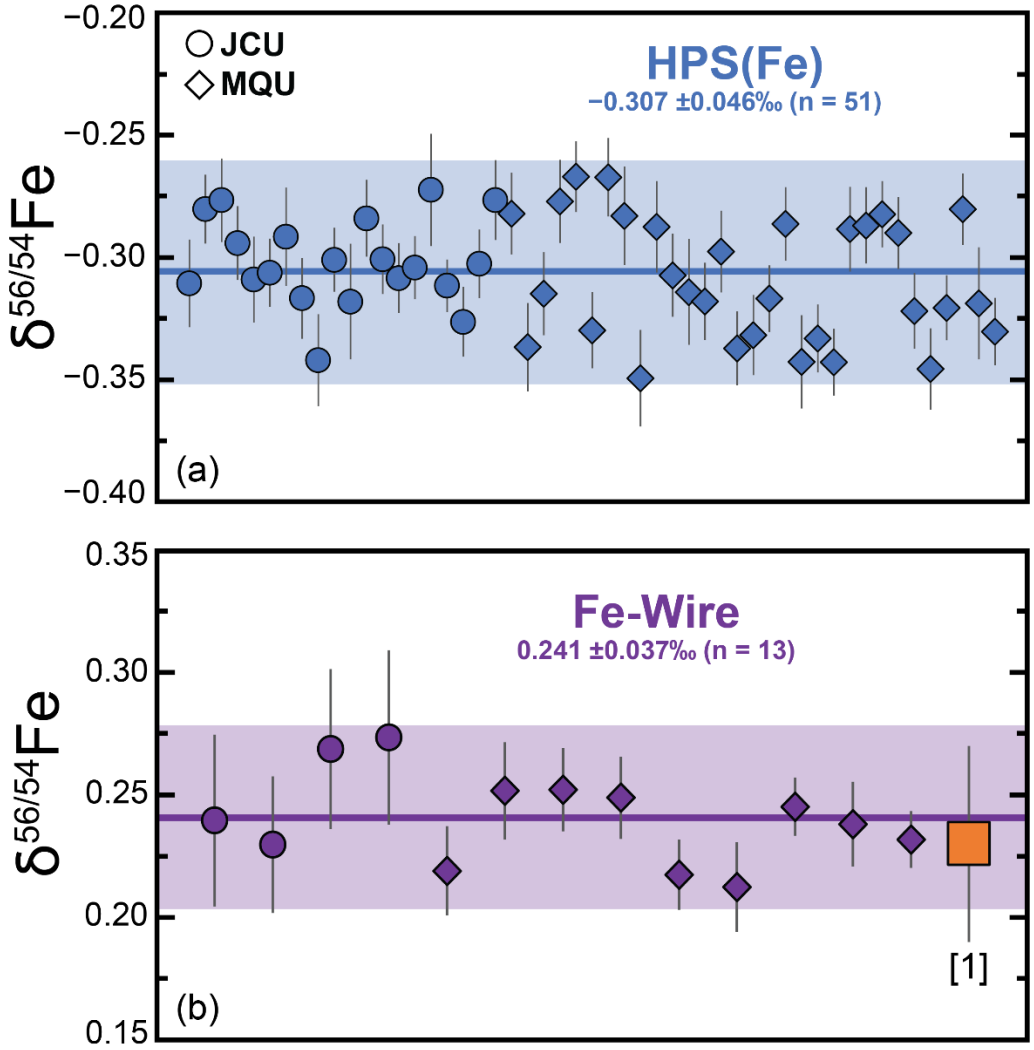

Figure S4: *Long-term instrument performance during MC-ICP-MS analyses over a 7-month period. Analyses were conducted at both JCU (circles) and MQU (diamonds). (a) Fe isotope composition of HPS Fe solution; (b) Fe isotope composition of Fe-Wire solution. Uncertainty bars are measured 2 standard error values, shaded fields represent average value (line) ± 2 standard deviations. Orange squares represent published values: 1) $\delta^{56}Fe$ = +0.23 ± 0.04 ‰ (Gerrits et al., 2019).*

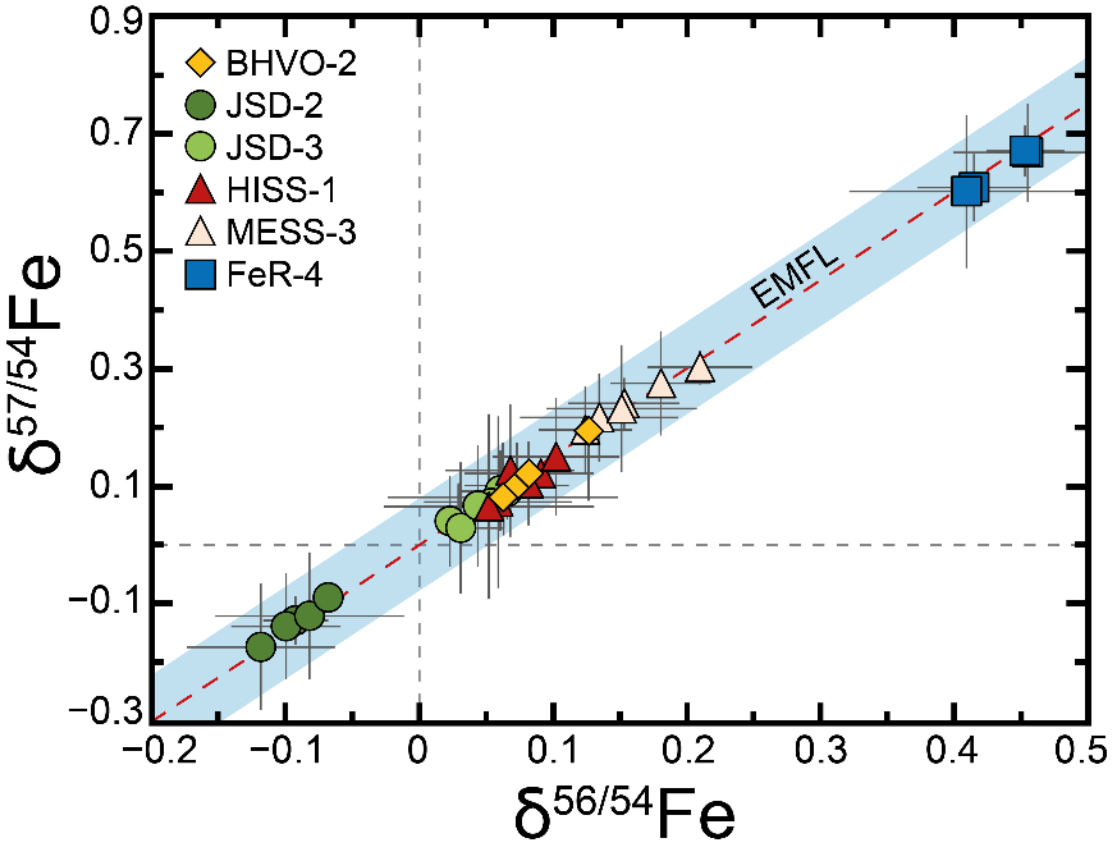

Figure S5: *Plot showing the mass dependent covariation between δ56Fe and δ57Fe of international rock standards measured in this study. Uncertainty bars represent 2 SD. The red dashed line represents the theoretical equilibrium mass-dependent fractionation line (EMFL; where the slope = 1.5014 is related to the relative atomic mass difference between the two isotope pairs (i.e. $\delta^{57}Fe = \delta^{56}Fe \times 1.5014$)). The shaded field represents the long-term repeatability of $\delta^{56}Fe$ of ± 0.05 ‰. All analyses exhibit mass dependence.*

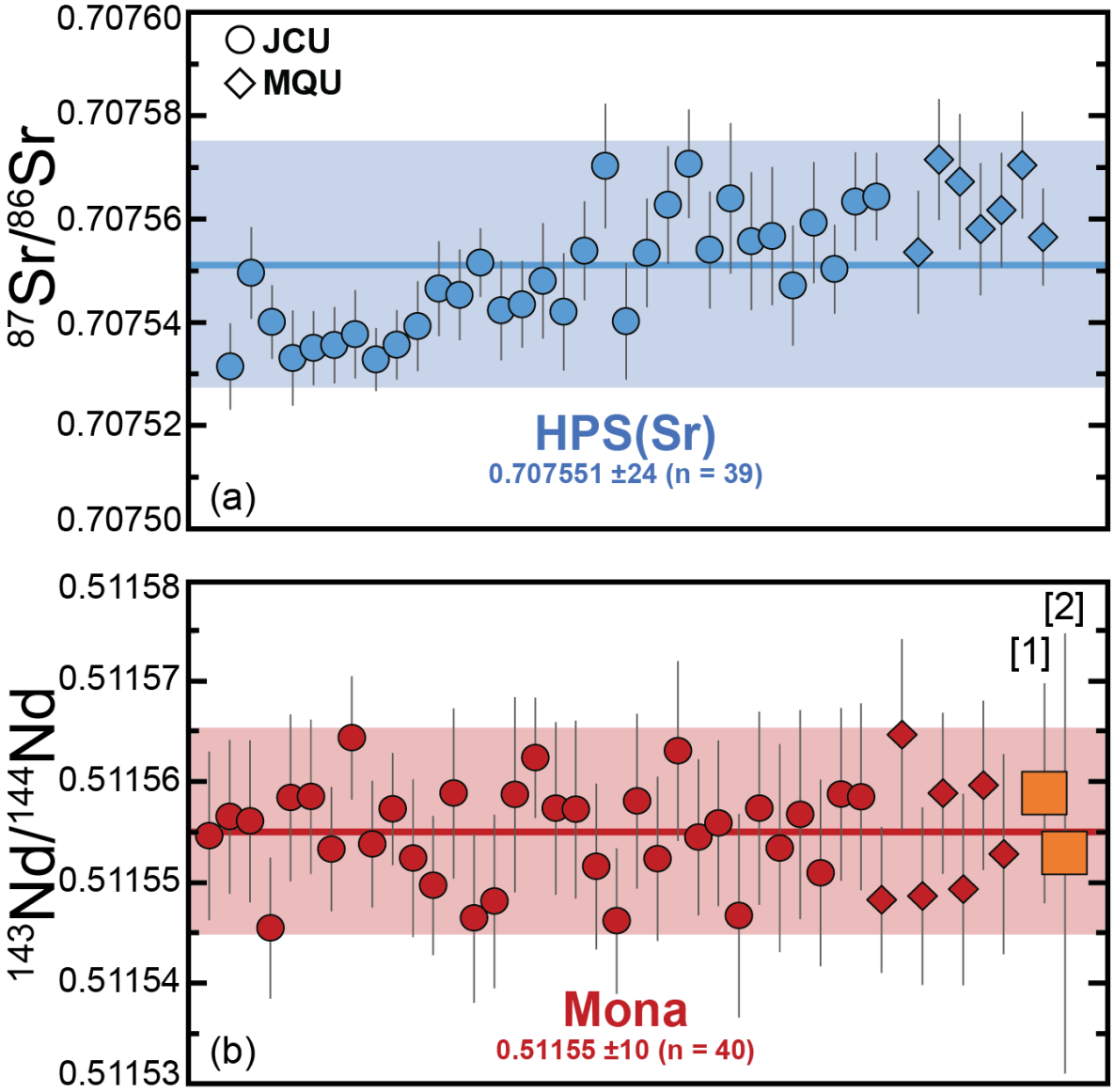

Figure S6: *Long-term instrument performance during MC-ICP-MS analyses over a 7-month period. Analyses were conducted at both JCU (circles) and MQU (diamonds). (a) Sr isotope composition of HPS Sr solution; (b) Nd isotope composition of Mona Nd solution. Uncertainty bars are measured 2 standard error values, shaded fields represent average value (line) ± 2 standard deviations. Orange squares represent published values: 1) $^{143}Nd/^{144}Nd$ = 0.511559 ± 11 (McCoy-West et al., 2020); 2) $^{143}Nd/^{144}Nd$ = 0.511553 ± 22 (Kaufmann & McCoy-West, 2025)*

2. Trace element data considerations

2.1 Anomalies in trace element data set

The analyses of sedimentary RM herein generally agree within ±10% for the majority of elements to previously published values (Bau & Alexander, 2009; Chauvel et al., 2011; Dulski, 2001; Fiket et al., 2017; Govindaraju, 1994; Imai et al., 1996; Kumakura et al., 2004; Outridge et al., 2017; Révillon & Hureau-Mazaudier, 2009; Roje, 2019; Sampaio & Enzweiler, 2015; Shaheen & Fryer, 2011; Waheed et al., 2007), although, some rare exceptions do exist. For example:

1) Zn concentrations for the majority of sedimentary RM (e.g. JSd-2, JSd-3, FeR-4, MESS-3) are consistently and often significantly lower (15-50 %) than those obtained in previous determinations, we attribute this to stringent contaminant reduction herein, including positive pressure HEPA-filtered chambers and the exclusive use of rinsed vinyl gloves which have the lowest inherit contamination from Zn (Garçon et al., 2017);

2) For JSd-2, nearly all REE concentrations are consistent with literature values within ±5 % (Chauvel et al., 2011; Dulski, 2001), with the exception of the elevated Eu consistently measured for JSd-2 (n = 5). Given that Eu concentrations for both BHVO-2 and FeR-4 are in excellent agreement with literature values (Bau & Alexander, 2009; Dulski, 2001; Jochum et al., 2016), this anomalous value is not considered an analytical artefact. It is possible it could result from contamination of this split of JSd-2 at JCU (which is >15 years old), however this is considered unlikely as it has not noticeably affected any of the other trace elements or REE, and as such this could indicate natural variability between commercially available batches of JSd-2 (see further evidence with respect to isotopes);

3) Concentrations for the high field strength elements (HFSE; Zr, Hf) in the JGS composite stream sediments (JSd-2, JSd-3) are significantly underestimated (ca. 50% relative), this discrepancy suggests the incomplete digestion of zircon grains due to the conventional hotplate digestions undertaken herein. This approach was used to accommodate the large sample masses (c. 100 mg) digested to minimize intra-aliquot heterogeneity. In hindsight this incomplete digestion is not surprising given the JGS RM possess the largest particle size at ≤ 149 µm of any RM herein (Terashima et al., 1990). Notwithstanding the anomalous HFSE data all other elements are considered sufficiently accurate in the JGS RM (Table DR3), meaning hotplate digestions remain suitable for trace element characterisation in most instances. Additionally, this dataset reconfirms the necessity for a very fine rock-powder (ideally < 74 µm; 200 mesh) when undertaking hotplate digestion on unknown materials, especially if they are expected to be enriched with refractory phases, whereas if HFSE

characterisation is a priority an alternative digestion method should be considered (e.g. Révillon & Hureau-Mazaudier, 2009; Yu et al., 2001).

Elemental data that is considered of sub-optimal quality are noted in Table DR3 and should be treated with these caveats in mind during future use.

2.2 Rationale for including BHVO-2 as an unknown

Simultaneously obtaining accurate and precise concentrations for a comprehensive suite of trace elements is a non-trivial task (Eggins et al., 1997; Roje, 2019). The basalt BHVO-2 is at present (and to the best of our knowledge) the most extensively-characterized RM for trace elements in existence (e.g. GeoReM; Jochum et al., 2005). Given all the sedimentary RM measured here are either missing data for some elements (see Table DR3) or suffer from heterogeneity or rare digestion issues (see above) it is currently unviable to use them to assess the precision and accuracy of all 47 measured elements. Therefore, here we have also included separate digestions of BHVO-2 that were processed entirely separately as unknowns throughout the analytical procedure (i.e. independent digestions from those used for normalisation). These analyses represent the best-case scenario given the identical matrix match with the calibrating standard.

3. Analytical Methods

3.1 Laboratory environment, reagents, and materials

Unless otherwise specified, all sample preparation (weighing, digestion, chemical separation, and refluxing and dilutions for analyses) occurred in the IsoTropics Geochemistry Laboratory, James Cook University, in a temperature and humidity controlled positive-pressure ISO 7 geochemical clean laboratory, with all chemistry occurring inside ULPA-filtered chemical workstations (ISO 5 or better conditions). Acids used in this study (unless specified) were double-distilled HNO_3 or HCl (using Savillex DST-1000 distillation units derived from Merck Analytical Reagent grade) or obtained at ultra-high purity (HF, H_2O_2; Seastar Baseline grade) to ensure the lowest possible blanks. Acid dilutions were conducted using ultra-high purity water (≥18.2Ω resistance; hereafter MQ H_2O) produced through a Milli-Q 7015 system equipped with an IQ Element dispensing unit.

Care was taken to minimise any potential exogenous contamination during the analytical program. All sample handling during solution-based work was conducted exclusively with vinyl gloves (which have the lowest inherent contaminants; Garçon et al., 2017; Jaouen et al., 2020) which were additionally rinsed with MQ H_2O and dried with Verasoft wipes to further remove any manufacturing residues . After surfactant cleaning using warm MQ H_2O and Decon90, all consumables are rinsed thrice with MQ H_2O. Plastics (1.5, 2- or 5-mL vials, pipette tips, etc.), are room-temperature leached

with 2 molL^{-1} HNO_3 for a minimum of 10 days. After leaching, plastic consumables are again rinsed thrice with MQ H_2O, then dried on an enclosed, HEPA-filtered clean bench (Thermo HeraGuard ECO) and capped and stored for further use. All PFA beakers (7, 15, 22 or 30 mL) for samples digestion and chemical separations undergo multistage cleaning as follows (all cleaning occurs at 120 °C; times specified are minima): 1) batch cleaning in 6 molL^{-1} analytical grade HNO_3 overnight to digest any potential contamination both inside and outside vessels; 2) individual closed vessel cleaning in 16 molL^{-1} HNO_3 for 24 hours; 3) individual closed vessel cleaning in 4 molL^{-1} HNO3 + trace HF (to remove adsorbed high field strength elements) for 48 hours; 4) individual closed vessel cleaning in 6 molL^{-1} HCl for 48-72 hours.

3.2 Major and volatile element analyses

Major element compositions were determined using a PANalytical Axios Advanced XRF at CODES Analytical Laboratory, University of Tasmania using well established techniques (Robinson, 2003; Watson, 1996). A 2 g aliquot of dry powdered sample was ignited at 1000 °C in a muffle furnace for 12 hrs (overnight), with each sample weighed before and after ignition, with the mass loss used to calculate the loss on ignition (LOI) of the sample. Fusion discs (32 mm) were prepared at 1100 °C in a rocker furnace in 95% Pt-5% Au crucibles. Glass discs were made by adding 0.6 g of fresh (not ignited) rock powder, 5.4 g 12:22 flux (Lithium Tetraborate-Metaborate mix), with 0.1 mL of saturated $LiNO_3$ solution (with exact weights recorded). X-Rays were generated using a 4 kW Rh anode with elemental fluorescence measured using a gas flow proportional detector with P10 gas (10% methane in argon), a sealed Xe Duplex and scintillation counter. Major element data was calculated by comparison with a range of well calibrated reference standards. Sulfur can be measured when the glass discs are made with unignited powder. The S is oxidized in the presence of $LiNO_3$, so remains fixed in the sample.

Total nitrogen, carbon, hydrogen, and sulfur contents were determined at the Central Science Laboratory, University of Tasmania, using a Thermo FlashSmart Elemental Analyser. Between 2 and 10 mg of sample were weighed into tin capsules using a Sartorius Cubis II ultra-microbalance to the nearest ± 0.1 µg. Combustion of the pressed tin cups was achieved in ultra-high purity oxygen at 1000 ºC (flash combustion takes place at about 1300 ºC) using tungstic oxide on alumina as an oxidising agent followed by copper wires as a reducing agent.

3.3 Sample digestion

For each RM, 100 mg was carefully weighed out into acid leached round bottomed 15-30 mL Savillex PFA beakers for digestion. To break down organic compounds, an initial 2 mL 16 molL^{-1} HNO_3 + 1 mL 9.8 molL^{-1} H_2O_2 was added to the samples, which was allowed to degas at room temperature (caps in

place but not tightened) as required depending on the intensity of the reaction; once degassing had largely ceased, caps were tightened, and the RM refluxed overnight at 100 °C for at least 12 hours. This step was only necessary for the organic rich sedimentary standards, however, for consistency (e.g. procedural blanks; oxidation) it was done to all samples. The solution was then evaporated to dryness at 95 °C, and the sample refluxed with 2 mL 29 $molL^{-1}$ HF + 1 mL 16 $molL^{-1}$ HNO_3 on a hotplate at 110 °C for at least 48 hours. A further 3 mL 16 $molL^{-1}$ HNO_3 was added to the reflux (to limit insoluble fluoride formation), and the sample was then dried down overnight at 85 °C. The samples were then sequential refluxed in 5 mL of 6 $molL^{-1}$ HCl, and 8 mL 6 $molL^{-1}$ HNO_3 until complete dissolution of the sample was achieved. Final sample digests were evaporated and refluxed in 10 mL of 2 $molL^{-1}$ HNO_3 for stable storage prior to aliquoting for further work. Final sample solutions were checked for clarity to ensure no mineral precipitates were present.

3.4 Trace element analyses

Digested samples were diluted 25 times by taking 200 µL of sample and adding 4.8 mL of 2% HNO_3 to produce 0.2 mg/mL solutions for analysis. Both sample and calibration solutions were gravimetrically diluted. Solutions were then analysed using a Thermo Fisher iCAP-TQ triple quadrupole inductively-coupled plasma mass spectrometer (TQ-ICP-MS) coupled to a Cetac ASX-560 autosampler fitted with a custom HEPA-filtered enclosure. A 5-point calibration was conducted using calibration solutions (zero-point blank; 0.5 ng/mL, 2 ng/mL, 10 ng/mL, 25 ng/mL diluted from High Purity Standards 10 mg/L ICP-MS-68A combined Solutions A and B; Lot# 2133408-100). Each analysis was preceded by a 60 s washout time and consisted of 3 replicates of 5 sweeps where each sweep represents 0.1 s of dwell time on each of the following isotope masses: ^{7}Li, ^{9}Be, ^{31}P, ^{45}Sc, ^{48}Ti, ^{51}V, ^{52}Cr, ^{55}Mn, ^{59}Co, ^{60}Ni, ^{65}Cu, ^{66}Zn, ^{71}Ga, ^{73}Ge, ^{75}As, ^{85}Rb, ^{88}Sr, ^{89}Y, ^{90}Zr, ^{93}Nb, ^{97}Mo, ^{111}Cd, ^{115}In, ^{118}Sn, ^{121}Sb, ^{133}Cs, ^{138}Ba, ^{139}La, ^{140}Ce, ^{141}Pr, ^{143}Nd, ^{149}Sm, ^{153}Eu, ^{157}Gd, ^{159}Tb, ^{163}Dy, ^{165}Ho, ^{166}Er, ^{169}Tm, ^{172}Yb, ^{175}Lu, ^{178}Hf, ^{181}Ta, ^{182}W, ^{205}Tl, ^{208}Pb, ^{209}Bi, ^{232}Th, and ^{238}U. The Qtegra software package aids in the selection of the optimum analytical mode to determine the abundance of each element most accurately by minimising direct isobaric or polyatomic interferences. Both kinetic energy discrimination (e.g. KED-mode) and isotopic mass shifts with the addition of oxygen (e.g. TQ-mode) were utilised in this study to avoid problematic overlapping masses (analytical modes utilised for each element can be found in the data repository).

Variations in instrumental mass bias due to difference in sample matrix (i.e. leading to signal suppression) were corrected online using a 5 ng/mL High Purity Standards Ru solution (diluted from 1000 µg/mL solution, Lot# 1305924). To obtain final concentrations, procedural blanks were subtracted from raw concentrations, which were then gravimetrically corrected using recorded

dilution masses. To ensure accuracy and correct for residual fluctuations in sensitivity across the entire mass spectrum that remain following internal normalisation (e.g. Eggins et al., 1997), a secondary normalisation using a well-characterised primary RM was implemented comparable to those undertaken previously (e.g. Chauvel et al., 2011; McCoy-West et al., 2015; Russo et al., 2024). Here we utilised the recommended values of the extensively -characterized RM BHVO-2 (Jochum et al., 2016) as although it is not an ideal matrix match for the sedimentary RM it possesses the largest bibliography for all 47 trace elements investigated here. Final concentrations in unknowns were obtained by applying a linear drift correction to each individual element using bracketing analyses of a single digestion of BHVO-2 measured a maximum of every 8 analyses throughout an analytical session. This normalisation procedure ensures consistency between data obtained in multiple sessions over an extended period.

3.5 O isotope analyses

Oxygen isotope analyses were conducted at the Queen's Facility for Isotope Research (QFIR), Queen's University, Canada sporadically over a 2 year period. Samples were acidified prior to oxygen extraction to remove carbonates using 20% HCl (v/v) at room temperature until no reaction was observed. Samples were rinsed thrice using 18.2 MΩ MQ H_2O and oven-dried overnight at 100 °C. Oxygen was then extracted from c. 5 mg of silicate sample at 550-600°C according to the conventional BrF_5 procedure of Clayton and Mayeda (1963). Unknowns (RM including NBS-28 and alkali basalt OREAS 24P) were loaded into Ni bombs with excess BrF_5 and heated overnight. The liberated oxygen was converted to CO_2 via sublimation of a carbon rod (EMS, CVP grade) and analysed using the multiport of a dual inlet system on a Thermo-Finnigan Delta Plus XP Isotope Ratio Mass Spectrometer (IRMS). Analyses were conducted using the factory installed CO_2 configuration with masses 44, 45 and 46 measured on Faraday cups 2, 3 and 4, respectively. Each analysis consisted of 8 cycles, at 2500 mV intensity, in CO_2 gas configuration using Isodat 3.0. Sample gas was measured against a reference gas calibrated against Vienna Standard Mean Ocean Water (VSMOW) using a suite of international standards (NBS18, NBS19, NBS20 and NBS23). A ^{17}O correction using the SSH algorithm (Santrock et al., 1985) was applied to the measured values. Oxygen isotope compositions are reported using the delta (δ) notation in units of *per mil* (‰) relative to VSMOW, with $\delta^{18}O = [(^{18}O/^{16}O_{Sample} / {}^{18}O/^{16}O_{VSMOW}) -1] \times 1{,}000]$.

3.6 Fe chemical separation

Digested sample aliquots were calculated to obtain fractions with 100 µg of Fe (based on the XRF results), the required volume of sample was pipetted into a clean 7 mL PFA beakers and dried down at 95 °C. To ensure complete destruction of any residual organic molecules, Fe aliquots were attacked

repeatedly with concentrated HNO_3 and H_2O_2. First, 0.5 mL 16 $molL^{-1}$ HNO_3 + 0.5 mL 9.8 $molL^{-1}$ H_2O_2 was added to the samples, and they were refluxed overnight at 120 °C. The sample was then dried at 95 °C and whilst warm additional concentrated HNO_3 and H_2O_2 was added dropwise to the samples (c. 4 and 2 drops, respectively) and dried immediately at 95 °C, this step was repeated twice. This additional digestion step prior to chemical separation was found to be critical to generate mass dependent Fe isotope data in the organic-rich sedimentary materials.

Chemical isolation of Fe was conducted using established measurement procedures (Dauphas et al., 2004; McCoy-West et al., 2018; Whitworth et al., 2020; Williams et al., 2004). Sample aliquots were prepared as above, with the final dried aliquots converted to chloride form by refluxing in 2 mL of 6 $molL^{-1}$ HCl at 120 °C for at least 2 hr, then dried-down at 95 °C, and subsequently refluxed at 100 °C in 1mL of 6 $molL^{-1}$ HCl overnight. For ion exchange chromatography samples were then loaded onto Biorad Polyprep ion exchange columns containing 1 mL of Biorad AG1-X8 (200-400 mesh, chloride form) anionic resin to isolate Fe from all other elements (Fig. S1; Table S1). Matrix elements were eluted from the column with 8 mL of 6 $molL^{-1}$ HCl, and subsequently purified Fe collected in 4 mL of 0.1 $molL^{-1}$ HCl. Solutions were then dried down at 95 °C and subsequently refluxed thrice in concentrated HNO_3-H_2O_2 (c. 4 and 2 drops, respectively) and dried immediately at 95 °C to remove any residual organics. Samples were then refluxed in 5 mL 0.5 $molL^{-1}$ HNO_3 for a minimum of 2 hr (ideally overnight) in preparation for isotope ratio determination ($^{56}Fe/^{54}Fe$ and $^{57}Fe/^{54}Fe$). Measured total procedural blanks for Fe ranged from 0.05 – 0.23 µg of Fe, with a median of 0.07 µg and average of 0.10 µg (n = 10), this equates to ≤ 0.2% of the sample Fe (typically 100 µg), and therefore are considered negligible.

3.7 Fe isotope mass spectrometry

Iron isotope measurements ($^{56}Fe/^{54}Fe$ and $^{57}Fe/^{54}Fe$) were conducted using a ThermoFinnigan Neptune MC-ICP-MS housed in the Advanced Analytical Centre (AAC) at JCU (n = 56) or a ThermoFinnigan Neptune *Plus* MC-ICP-MS housed in the Macquarie Analytical Facility (MAF) at Macquarie University (MQU), Sydney (n = 135). For the most part, analyses on both instruments utilised the same sample introduction system (SIS) and data acquisition parameters, with the minor differences explained below. The SIS consisted of a double-pass cyclonic spray chamber (Glass Expansion) and an Elemental Scientific PFA-ST nebulizer with a 100 µL/min integrated probe-capillary assembly. Standard Ni sample and H-skimmer cones were used. Each analysis was preceded by a 60 second wash out and consisted of 40 cycles of 4 second integrations using static faraday collectors. Along with the isotopes of Fe (^{54}Fe, ^{56}Fe, ^{57}Fe, and ^{58}Fe), ^{53}Cr and ^{60}Ni were measured simultaneously to enable correction of direct isobaric interferences on ^{54}Fe and ^{58}Fe, respectively (Table S2). These

corrections were negligible due to the effective separation of Fe from Cr and Ni during column chromatography. Prior to analyses, Fe solutions were diluted 10 times, and the concentration was determined using the MC-ICP-MS based on the beam intensity of ^{56}Fe in the dilution relative to a known Fe solution (i.e. single-point voltage equivalence). Samples were then diluted as required to match the sample Fe intensities to that of standards. This step also allows confirmation of complete Fe yield following the chemical separation. In this study Fe yields were > 99% in all cases.

***Table S1**: Ion exchange chromatography procedures for separation of purified aliquots of Fe, Nd and Sr prior to isotopic measurements.*

	Iron (Fe)	Neodymium (Nd)	Strontium (Sr)
Resin	Anion	Cation	Sr-Spec
	1 mL AG1-x8	2 mL AGw50-x8	100 µL
Cleaning	10 mL 6 $molL^{-1}$ HCl	3 x 10 mL 6 $molL^{-1}$ HCl	2 x 1.5 mL MQ H_2O
	10 mL 0.5 $molL^{-1}$ HCl		2 x 1.5 mL 3 $molL^{-1}$ HNO_3
	10 mL 0.1 $molL^{-1}$ HCl		2 x 1.5 mL MQ H_2O
Conditioning	2 mL 6 $molL^{-1}$ HCl	4 mL 1.5 $molL^{-1}$ HCl	1 mL 3 $molL^{-1}$ HNO_3
Sample Loading	1 mL 6 $molL^{-1}$ HCl	1.9 mL 1.5 $molL^{-1}$ HCl	0.5 mL 3 $molL^{-1}$ HNO_3
Matrix Rinse	2 x 4 mL 6 $molL^{-1}$ HCl	8 mL 1.5 $molL^{-1}$ HCl + 0.2 $molL^{-1}$ HF	3 x 1.5 mL 3 $molL^{-1}$ HNO_3
		5 mL 1.5 $molL^{-1}$ HCl	
		12 mL 2.5 $molL^{-1}$ HCl^	
		10 mL 2 $molL^{-1}$ HNO_3	
Analyte Collection	4 mL 0.1 $molL^{-1}$ HCl	13 mL 6 $molL^{-1}$ HCl*	2 x 1.5 mL MQ H_2O

^2.5 molL-1 HCl fraction collected from Cation column is then further purified using Sr-Spec column
*Neodymium fraction is a total rare earth element fraction.

An additional complication when measuring Fe isotopes are the direct polyatomic isobaric interferences generated in the Ar plasma. These interferences include $^{40}Ar^{14}N$, $^{40}Ar^{16}O$, $^{40}Ar^{16}O^{1}H$, and $^{40}Ar^{18}O$ on ^{54}Fe, ^{56}Fe, ^{57}Fe, and ^{58}Fe, respectively (Table S2). Given these interferences are produced in the instrument, they must be resolved by increasing the mass resolution and measuring iron isotopes as flat-topped peak shoulders in medium- or high-resolution mode (MR and HR; respectively). In this study care was taken to ensure the mass resolution was > 8000 on the plateau of ^{56}Fe (where resolution = m/[m(95%) – m(5%)]). This was achieved using slightly different approaches, as required

due to the operating efficiency of the different instruments at the time of their usage. Iron isotope measurements conducted using the Neptune MC-ICP-MS at JCU were performed in HR mode, this required analyte solution with an Fe concentration of 9 µg/mL to obtain sufficiently large beams on ^{56}Fe > 35V to ensure voltages on the less abundant isotopes were high enough for precise data acquisition. Iron isotope measurements on the Neptune *Plus* MC-ICP-MS at MQU were instead performed in MR mode, requiring analyte solutions with an Fe concentration of 4.5 µg/mL to produce comparable signal intensities. All data in this study were calculated using the standard-sample bracketing (SSB) method (Dauphas et al., 2009; Maréchal et al., 1999; McCoy-West et al., 2024; McCoy-West et al., 2018). The internationally recognized Fe isotope standard IRMM-524B, which has an isotope composition identical to the exhausted IRMM-014 (Craddock & Dauphas, 2011), was used as the bracketing standard throughout the analytical campaign. All results are reported relative to the IRMM-524B standard with $\delta^{56}Fe = [(^{56}Fe/^{54}Fe_{Sample} / {}^{56}Fe/^{54}Fe_{IRMM524B}) -1] \times 1{,}000]$ where $^{56}Fe/^{54}Fe_{IRMM524B}$ corresponds to the average composition of the two bracketing standard measurements immediately before and after the measurement of the unknown sample (the same formula applies for $\delta^{57}Fe$, however, the $^{57}Fe/^{54}Fe$ ratio is used instead).

The determination of accurate transition metal stable isotope ratios when implementing the SSB method, as is the case in this study, requires stable instrumental mass bias. Variations in instrumental mass bias are generally the result of fluctuations in the plasma, which can be attributed to differences in the analyte load during sample introduction. In this study, stringent quality control criteria formalised here were applied to the entire dataset. The following rejection filter was applied to the individual measurements that make up the reported data: 1) the measured intensity (voltage) of ^{56}Fe in the unknown solution was within 10% of that for the bracketing standards; 2) the mass bias related mass spectrometer drift observed between the bracketing IRMM 524B standards was ≤ 0.10 ‰; 3) the $\delta^{56}Fe$ and $\delta^{57}Fe$ data were mass dependent within 1.5 times of the measured individual analytical uncertainties of that measurement.

***Table S2**: Faraday cup configurations used for MC-ICP-MS Fe, Sr and Nd isotope measurements, showing important isobaric and polyatomic interferences.*

Cup	L4	L3	L2	L1	Ax	H1	H2	H3	H4
<u>Iron</u>									
Analyte Isotopes	^{53}Cr		^{54}Fe		^{56}Fe	^{57}Fe	^{58}Fe		^{60}Ni
Isobars			^{54}Cr				^{58}Ni		
Polyatomic			$^{40}Ar^{14}N$		$^{40}Ar^{16}O$	$^{40}Ar^{16}O^{1}H$	$^{40}Ar^{18}O$		
<u>Strontium</u>									

Analyte Isotopes	^{82}Kr	^{83}Kr	^{84}Sr	^{85}Rb	^{86}Sr	^{87}Sr	^{88}Sr		
Isobars			^{84}Kr		^{86}Kr	^{87}Rb			
Neodymium									
Analyte Isotopes	^{142}Nd	^{143}Nd	^{144}Nd	^{145}Nd	^{146}Nd	^{147}Sm	^{148}Nd	^{149}Sm	^{150}Nd
Isobars	^{142}Ce		^{144}Sm				^{148}Sm		^{150}Sm

3.8 Nd-Sr chemical separation

Following trace element quantification, RM aliquots were calculated based on TQ-ICP-MS results and prepared to generate 1 µg of Nd (Nd occurs in lower concentration than Sr and therefore is the limiting analyte). Calculated sample aliquots were dried at 95 °C, converted to chloride form by refluxing in 2 mL of 6 molL^{-1} HCl at 120 °C for at least 2 hr, then dried-down at 95 °C. Chemical separation of Nd and Sr was conducted using a two column procedure (Fig. S1; Table S1) that is based on well-established measurement procedures that have been optimised over a 10 year period utilising cation exchange resin for Nd purification and Sr-Spec resin for Sr purification (e.g. McCoy-West et al., 2010; McCoy-West et al., 2016; McCoy-West et al., 2022).

The ability of cation specific resins to achieve excellent separation of the REE from other matrix elements in silicate rocks has long been recognised (e.g. Strelow, 1960; Watkins & Nolan, 1992). BioRad Polyprep columns were loaded with 2 mL of BioRad AG50W-X8 (100-200 mesh; chloride form) cationic resin and cleaned repeatedly with 3 x 10 mL of 6 molL^{-1} HCl. Aliquots were bought into solution in 1.9 mL of 1.5M HCl and refluxed at 100 °C for a minimum of 2 hr (ideally overnight) in preparation for loading onto the column. The solutions were transferred into leached 2 mL polypropylene vials and centrifuged for 5 min at 12 000 rpm, prior to carefully loading the supernatant onto the columns (i.e. avoiding any precipitate; very rare). This step is required as these columns can be reused numerous times (> 15) over several years if the analyst is careful. Following sample loading matrix elements were sequentially eluted from the column with 2 mL of 1.5 molL^{-1} HCl, 8 mL of 1.5 molL^{-1} HCl + 0.2 molL^{-1} HF, and 5 mL of 1.5 molL^{-1} HCl (Table S1). Partially purified Sr fractions were then collected using 12 mL of 2.5 molL^{-1} HCl into leached 15 mL PFA beakers and dried-down overnight at 95 °C. Next an additional matrix wash with 10 mL of 2 molL^{-1} HNO_3 was undertaken to remove Ba, which can interfere during mass spectrometry. Finally, the REE (including Nd) were then collected together in 13 mL of 6 molL^{-1} HCl into another leached 15 mL PFA beaker. This REE fraction was of sufficient purity that robust Nd isotopic analyses were possible on these fractions without further separation chemistry. REE isolate solutions were dried-down overnight at 95 °C, then refluxed with concentrated HNO_3-H_2O_2 (c. 4 and 2 drops, respectively) and dried

immediately at 95 °C to breakdown any residual organics. Final dried sample isolates were refluxed in 2 mL of 0.5 $molL^{-1}$ HNO_3 for a minimum of 2 hr (ideally overnight), so they contained c. 500 ng/mL of Nd in preparation for mass spectrometry. Measured total procedural blanks for Nd ranged from 0.01 – 0.85 ng (n = 8), with an average of 0.41 ng and a significantly lower median of 0.07 ng. The contribution of the blanks typical equates to ≤ 0.5% of sample Nd (typically 1000 ng), and therefore they have negligible influence on the measured isotope values.

Further Sr purification (Fig. S1) was conducted using columns filled with the highly selective Sr specific resin (e.g. Charlier et al., 2006; De Muynck et al., 2009; Horwitz et al., 1992). Custom ion exchange columns made from clear polypropylene 1 mL pipette tips (Thermo Scientific FinnTips; with the bottom 3 mm of the tip removed) using 4 x 1.6 mm Biocomma hydrophillic frits and were subsequently filled with c. 100 µL of pre-cleaned Eichrom Sr-spec resin (50-100 µm; c. 4-5 mm resin bed thickness). The Sr-Spec resin, rather than any reagents, is the major source of contamination during this procedure (e.g. Charlier et al., 2006) due to its excellent ability to retain Sr. Therefore 20 mL of Sr-Spec Resin was batched cleaned using a BioRad 30 mL Econo-Pac column topped with a 250 mL Econo-Column Funnel, the resin was sequentially cleaned with MQ H_2O x 3, 8 $molL^{-1}$ HNO_3, 3 $molL^{-1}$ HNO_3, 0.5 $molL^{-1}$ HNO_3, MQ H_2O, 6 $molL^{-1}$ HCl, 0.5 $molL^{-1}$ HCl, and MQ H_2O x 3, prior to storage in 0.5 $molL^{-1}$ HNO_3. In this instance, due to the organic-rich nature of the sedimentary samples this was topped with c. 50 µL (c. 2 mm resin bed thickness) of Triskem prefilter resin (50-100 µm) to help sequester organic compounds and ensure the efficient operation of the Sr-Spec resin. Once loaded columns were sequentially cleaned twice with MQ H_2O, 3 $molL^{-1}$ HNO_3 and MQ H_2O (Table S1). Dried Sr fractions collected from the cation columns were converted to nitrite form by adding 5 drops of 16 $molL^{-1}$ HNO_3 and drying immediately at 95 °C and then refluxing in 0.5 mL of 3 $molL^{-1}$ HNO_3 at 100 °C for at least 2 hr (ideally overnight) and then loaded onto the Sr-Spec columns. Column chromatography was conducted using leached FEP squeeze bottles. The remaining matrix elements (e.g. Ca, Rb) washed from the column using 3 column volumes (c. 4.5 mL) of 3 $molL^{-1}$ HNO_3, Sr was then eluted in 2 column volumes (c. 3 mL) of MQ H_2O into acid-leached PFA vials. Purified Sr solutions were dried-down at 95 °C, then refluxed with concentrated HNO_3-H_2O_2 (c. 4 and 2 drops, respectively) and dried immediately at 95 °C to breakdown any residual organics. Final dried Sr isolates were refluxed at 100 °C in 1 mL of 0.5 $molL^{-1}$ HNO_3 for a minimum of 2 hr (ideally overnight) in preparation for mass spectrometry. Measured total procedural blanks for Sr ranged from 0.04 – 1.19 ng of Sr, with a median of 0.37 ng and average of 0.54 ng (n = 11), this equates to ≤ 0.1% of sample Sr (typical > 2000 ng) and therefore is considered negligible.

3.9 Sr isotope mass spectrometry

Strontium isotope measurements (radiogenic $^{87}Sr/^{86}Sr$) were conducted using a Neptune MC-ICP-MS at JCU (n = 65) or a Neptune Plus MC-ICP-MS at MQU (n = 14). Sr solutions were diluted 10 times for concentration checking and diluted as required so the analysed solutions contained 500 ng/mL of Sr. Analyses on both instruments utilised the same SIS and data acquisition parameters. The SIS consisted of a double-pass cyclonic spray chamber (Glass Expansion) and an Elemental Scientific PFA-ST nebulizer with a 50 µL/min integrated probe-capillary assembly. Standard Ni sample and H-skimmer cones were used. Measurements were performed in low mass resolution (LR mode). Each analysis was preceded by a 90 second wash out and consisted of 50 cycles of 4 second integrations with static faraday collectors (Table S2). Sr isotope ratios were mass bias corrected using a $^{86}Sr/^{88}Sr$ ratio of 0.1194. The Sr isotope standard NIST SRM 987 was used to monitor instrument stability and correct for intra-session variations with all data reported relative to a $^{87}Sr/^{86}Sr$ value of SRM 987 = 0.710248 (Thirlwall, 1991).

3.10 Nd isotope mass spectrometry

Neodymium isotope measurements (radiogenic $^{143}Nd/^{144}Nd$) were conducted using a Neptune MC-ICP-MS at JCU (n = 79) or a Neptune Plus MC-ICP-MS housed at MQU (n = 10). Analyses on both instruments utilised the same SIS and data acquisition parameters. The SIS consisted of a double-pass cyclonic spray chamber (Glass Expansion) and an Elemental Scientific PFA-ST nebulizer with a 50 µL/min integrated probe-capillary assembly. Standard Ni sample and H-skimmer cones were used. Measurements were performed in low mass resolution (LR mode). Each analysis was preceded by a 90 second wash out and consisted of 50 cycles of 4 second integrations using static faraday collectors (Table S2). The chemical separation procedure implemented above made no attempt to separate Nd from Sm. Therefore, online correction for the presence of direct isobaric interferences from Sm (on ^{144}Nd, ^{148}Nd and ^{150}Nd) was conducted using mass bias corrected Sm intensities based on the measured the $^{149}Sm/^{147}Sm$ ratio and a normalization ratio of 0.9216 (Wasserburg et al., 1981). Nd isotope ratios were then mass bias corrected using the Sm interference free $^{146}Nd/^{145}Nd$ ratio using a value of 2.071943 (equivalent to the widely used $^{146}Nd/^{144}Nd$ ratio of 0.7219). This type of correction is commonly applied during in-situ Nd isotope measurements (e.g. Doucelance et al., 2020; Spandler et al., 2016) due to its ability to effectively remove analytical artefacts. To ensure the validity of these correction procedures, all primary and secondary standards were also doped with an in-house Alfa Aesar Specpure 1000 µg/mL Sm solution (Lot# 227269F) at approximately the chondritic Nd-Sm ratio (Nd = 500 ng/mL; Sm = 200 ng/mL) as would be expected in the unknowns to confirm the accuracy of the correction procedure. The internationally recognized Nd isotope standard JNdi-1 was used to

monitor instrument stability and correct for intra-session variations with all data reported relative to a $^{143}Nd/^{144}Nd$ value of JNdi-1 = 0.512115 (Tanaka et al., 2000).

3.11 Comparison of multi-collector instruments

The Fe, Sr and Nd isotope determinations measurements undertaken here were conducted across a 8-month period and completed on two different instruments in separate cities: 1) Neptune MC-ICP-MS at the Advanced Analytical Centre, JCU, Townsville; and 2) Neptune Plus MC-ICP-MS at the Macquarie Analytical Facility, MQU, Sydney. Undertaking analyses on two distinct generations of instrument housed at different institutions, that ultimately produced results within uncertainty, further validates the robustness of the dataset presented. Noting both instruments were not used for the same length of time or equally to undertake the different isotope analyses (e.g. Sr, Nd and Fe). Ultimately, as shown in Figures S4 and S5 for a range of synthetic standards the two instruments generated isotopic compositions that are within uncertainty of each other. By looking in detail at analyses of individual RM (e.g. JSd-2) provided in the data repository (Tables DR6-DR8), when heterogeneity is not an issue (see discussion in main text) the same isotopic compositions are obtained with all data generated at JCU and MQU within analytical uncertainty.

References

Baker, J. A., Macpherson, C. G., Menzies, M. A., Thirlwall, M. F., Al-Kadasi, M., & Mattey, D. P. (2000). Resolving crustal and mantle contributions to continental flood volcanism, Yemen: constraints from mineral oxygen isotope data. *Journal of Petrology*, *41*(12), 1805-1820. https://doi.org/10.1093/petrology/41.12.1805

Bau, M., & Alexander, B. W. (2009). Distribution of high field strength elements (Y, Zr, REE, Hf, Ta, Th, U) in adjacent magnetite and chert bands and in reference standards FeR-3 and FeR-4 from the Temagami iron-formation, Canada, and the redox level of the Neoarchean ocean. *Precambrian Research*, *174*(3), 337-346. https://doi.org/https://doi.org/10.1016/j.precamres.2009.08.007

Charlier, B. L. A., Ginibre, C., Morgan, D., Nowell, G. M., Pearson, D. G., Davidson, J. P., & Ottley, C. J. (2006). Methods for the microsampling and high-precision analysis of strontium and rubidium isotopes at single crystal scale for petrological and geochronological applications. *Chemical Geology*, *232*(3–4), 114-133. https://doi.org/http://dx.doi.org/10.1016/j.chemgeo.2006.02.015

Chauvel, C., Bureau, S., & Poggi, C. (2011). Comprehensive Chemical and Isotopic Analyses of Basalt and Sediment Reference Materials. *Geostandards and Geoanalytical Research*, *35*(1), 125-143. https://doi.org/https://doi.org/10.1111/j.1751-908X.2010.00086.x

Clayton, R. N., & Mayeda, T. K. (1963). The use of bromine pentafluoride in the extraction of oxygen from oxides and silicates for isotopic analysis. *Geochimica et Cosmochimica Acta*, *27*(1), 43-52. https://doi.org/https://doi.org/10.1016/0016-7037(63)90071-1

Craddock, P. R., & Dauphas, N. (2011). Iron isotopic compositions of geological reference materials and chondrites. *Geostandards and Geoanalytical Research*, *35*(1), 101-123. https://doi.org/https://doi.org/10.1111/j.1751-908X.2010.00085.x

Dauphas, N., Janney, P. E., Mendybaev, R. A., Wadhwa, M., Richter, F. M., Davis, A. M., van Zuilen, M., Hines, R., & Foley, C. N. (2004). Chromatographic Separation and Multicollection-ICPMS Analysis of Iron. Investigating Mass-Dependent and -Independent Isotope Effects. *Analytical Chemistry*, *76*(19), 5855-5863. https://doi.org/10.1021/ac0497095

Dauphas, N., Pourmand, A., & Teng, F.-Z. (2009). Routine isotopic analysis of iron by HR-MC-ICPMS: How precise and how accurate? *Chemical Geology*, *267*(3), 175-184. https://doi.org/https://doi.org/10.1016/j.chemgeo.2008.12.011

De Muynck, D., Huelga-Suarez, G., Van Heghe, L., Degryse, P., & Vanhaecke, F. (2009). Systematic evaluation of a strontium-specific extraction chromatographic resin for obtaining a purified Sr fraction with quantitative recovery from complex and Ca-rich matrices [10.1039/B908645E]. *Journal of Analytical Atomic Spectrometry*, *24*(11), 1498-1510. https://doi.org/10.1039/B908645E

Doucelance, R., Bruand, E., Matte, S., Bosq, C., Auclair, D., & Gannoun, A.-M. (2020). In-situ determination of Nd isotope ratios in apatite by LA-MC-ICPMS: Challenges and limitations. *Chemical Geology*, *550*, 119740. https://doi.org/https://doi.org/10.1016/j.chemgeo.2020.119740

Dulski, P. (2001). Reference Materials for Geochemical Studies: New Analytical Data by ICP-MS and Critical Discussion of Reference Values. *Geostandards Newsletter*, *25*(1), 87-125. https://doi.org/https://doi.org/10.1111/j.1751-908X.2001.tb00790.x

Eggins, S. M., Woodhead, J. D., Kinsley, L. P. J., Mortimer, G. E., Sylvester, P., McCulloch, M. T., Hergt, J. M., & Handler, M. R. (1997). A simple method for the precise determination of ≥ 40 trace elements in geological samples by ICPMS using enriched isotope internal standardisation. *Chemical Geology*, *134*(4), 311-326. https://doi.org/https://doi.org/10.1016/s0009-2541(96)00100-3

Fiket, Ž., Mikac, N., & Kniewald, G. (2017). Mass Fractions of Forty-Six Major and Trace Elements, Including Rare Earth Elements, in Sediment and Soil Reference Materials Used in

Environmental Studies. *Geostandards and Geoanalytical Research*, *41*(1), 123-135. https://doi.org/https://doi.org/10.1111/ggr.12129

Garçon, M., Sauzéat, L., Carlson, R. W., Shirey, S. B., Simon, M., Balter, V., & Boyet, M. (2017). Nitrile, Latex, Neoprene and Vinyl Gloves: A Primary Source of Contamination for Trace Element and Zn Isotopic Analyses in Geological and Biological Samples. *Geostandards and Geoanalytical Research*, *41*(3), 367-380. https://doi.org/https://doi.org/10.1111/ggr.12161

Gerrits, A. R., Inglis, E. C., Dragovic, B., Starr, P. G., Baxter, E. F., & Burton, K. W. (2019). Release of oxidizing fluids in subduction zones recorded by iron isotope zonation in garnet. *Nature Geoscience*, *12*(12), 1029-1033. https://doi.org/10.1038/s41561-019-0471-y

Govindaraju, K. (1994). Compilation of working values and sample description for 383 geostandards. *Geostandards Newsletter*, *18*, 1-158. https://doi.org/https://doi.org/10.1046/j.1365-2494.1998.53202081.x-i1

Horwitz, P. E., Renato, C., & L., M. D. (1992). A novel strontium-selective extraction chromotographic resin. *Solvent Extraction and Ion Exchange*, *10*(2), 313-336. https://doi.org/10.1080/07366299208918107

Hou, S., Yang, S., Sun, J., & Ding, Z. (2003). Oxygen isotope compositions of quartz grains (4–16 μm) from Chinese eolian deposits and their implications for provenance. *Science in China Series D: Earth Sciences*, *46*(10), 1003-1011. https://doi.org/10.1007/BF02959395

Imai, N., Terashima, S., Itoh, S., & Ando, A. (1996). Compilation of analytical data on nine GSJ geochemical reference samples, "Sedimentary Rock Series". *Geostandards Newsletter*, *20*(2), 165-216. https://doi.org/https://doi.org/10.1111/j.1751-908X.1996.tb00184.x

Jaouen, K., Trost, M., Bourgon, N., Colleter, R., Le Cabec, A., Tütken, T., Elias Oliveira, R., Pons, M. L., Méjean, P., Steinbrenner, S., Chmeleff, J., & Strauss, A. (2020). Zinc isotope variations in archeological human teeth (Lapa do Santo, Brazil) reveal dietary transitions in childhood and no contamination from gloves. *PLOS ONE*, *15*(5), e0232379. https://doi.org/10.1371/journal.pone.0232379

Jochum, K. P., Nohl, U., Herwig, K., Lammel, E., Stoll, B., & Hofmann, A. W. (2005). GeoReM: A new geochemical database for reference materials and isotopic standards. *Geostandards and Geoanalytical Research*, *29*(3), 333-338. https://doi.org/10.1111/j.1751-908X.2005.tb00904.x

Jochum, K. P., Weis, U., Schwager, B., Stoll, B., Wilson, S. A., Haug, G. H., Andreae, M. O., & Enzweiler, J. (2016). Reference Values Following ISO Guidelines for Frequently Requested Rock Reference Materials. *Geostandards and Geoanalytical Research*, *40*(3), 333-350. https://doi.org/10.1111/j.1751-908X.2015.00392.x

Kaufmann, A. K. C., & McCoy-West, A. J. (2025). Combined Stable and Radiogenic Nd Isotope Characterisation of Sedimentary and Iron Formation Reference Materials by Double Spike MC-ICP-MS. *Geostandards and Geoanalytical Research*, *n/a*(n/a). https://doi.org/https://doi.org/10.1111/ggr.70020

Kubota, R. (2009). Simultaneous Determination of Total Carbon, Nitrogen, Hydrogen and Sulfur in Twenty-seven Geological Reference Materials by Elemental Analyser. *Geostandards and Geoanalytical Research*, *33*(2), 271-283. https://doi.org/https://doi.org/10.1111/j.1751-908X.2009.00905.x

Kumakura, S., Tanaka, M., Hashimoto, S., & Maeda, M. (2004). Determination of lanthanides and heavy metals in Sagami Bay sediment and sediment reference material MESS-3. *Bunseki Kagaku*, *53*(10), 1101-1104. https://doi.org/10.2116/bunsekikagaku.53.1101

Maréchal, C. N., Télouk, P., & Albarède, F. (1999). Precise analysis of copper and zinc isotopic compositions by plasma-source mass spectrometry. *Chemical Geology*, *156*(1–4), 251-273. https://doi.org/http://dx.doi.org/10.1016/S0009-2541(98)00191-0

McCoy-West, A. J., Baker, J. A., Faure, K., & Wysoczanski, R. (2010). Petrogenesis and origins of mid-Cretaceous continental intraplate volcanism in Marlborough, New Zealand: Implications for

the long-lived HIMU magmatic mega-province of the SW Pacific. *Journal of Petrology*, *51*(10), 2003-2045. https://doi.org/10.1093/petrology/egq046

McCoy-West, A. J., Bennett, V. C., & Amelin, Y. (2016). Rapid Cenozoic ingrowth of isotopic signatures simulating "HIMU" in ancient lithospheric mantle: Distinguishing source from process. *Geochimica et Cosmochimica Acta*, *187*, 79-101. https://doi.org/http://dx.doi.org/10.1016/j.gca.2016.05.013

McCoy-West, A. J., Bennett, V. C., O'Neill, H. S. C., Hermann, J., & Puchtel, I. S. (2015). The interplay between melting, refertilization and carbonatite metasomatism in off-cratonic lithospheric mantle under Zealandia: An integrated major, trace and platinum group element study. *Journal of Petrology*, *56*(3), 563-604. https://doi.org/10.1093/petrology/egv011

McCoy-West, A. J., Davis, A. M., Wainwright, A. N., & Tomkins, A. G. (2024). Simplifying silver isotope analysis of metallic samples: using silver nitrate precipitation to avoid perilous chloride formation [10.1039/D3JA00374D]. *Journal of Analytical Atomic Spectrometry*. https://doi.org/10.1039/D3JA00374D

McCoy-West, A. J., Godfrey Fitton, J., Pons, M.-L., Inglis, E. C., & Williams, H. M. (2018). The Fe and Zn isotope composition of deep mantle source regions: Insights from Baffin Island picrites. *Geochimica et Cosmochimica Acta*, *238*, 542-562. https://doi.org/https://doi.org/10.1016/j.gca.2018.07.021

McCoy-West, A. J., Millet, M.-A., Nowell, G. M., Nebel, O., & Burton, K. W. (2020). Simultaneous measurement of neodymium stable and radiogenic isotopes from a single aliquot using a double spike [10.1039/C9JA00308H]. *Journal of Analytical Atomic Spectrometry*, *35*(2), 388-402. https://doi.org/10.1039/C9JA00308H

McCoy-West, A. J., Mortimer, N., Burton, K. W., Ireland, T. R., & Cawood, P. A. (2022). Re-initiation of plutonism at the Gondwana margin after a magmatic hiatus: The bimodal Permian-Triassic Longwood Suite, New Zealand. *Gondwana Research*, *105*, 432-449. https://doi.org/https://doi.org/10.1016/j.gr.2021.09.021

Outridge, P. M., Sanei, H., Courtney Mustaphi, C. J., & Gajewski, K. (2017). Holocene climate change influences on trace metal and organic matter geochemistry in the sediments of an Arctic lake over 7,000 years. *Applied Geochemistry*, *78*, 35-48. https://doi.org/https://doi.org/10.1016/j.apgeochem.2016.11.018

Reed, W. P. (1992). Certificate of analysis NISTSRM8546.

Révillon, S., & Hureau-Mazaudier, D. (2009). Improvements in Digestion Protocols for Trace Element and Isotope Determinations in Stream and Lake Sediment Reference Materials (JSd-1, JSd-2, JSd-3, JLk-1 and LKSD-1). *Geostandards and Geoanalytical Research*, *33*(3), 397-413. https://doi.org/https://doi.org/10.1111/j.1751-908X.2009.00008.x

Robinson, P. (2003). XRF and laser ablation ICP-MS analysis of flux-fused discs. Geoanalysis 2003. 5th International conference on the analysis of geological and environmental materials Rovaniemi, Finland.

Roje, V. (2019). Comment on: Mass Fractions of Forty-Six Major and Trace Elements, Including Rare Earth Elements, in Sediment and Soil Reference Materials Used in Environmental Studies. Fiket et al. (2017), Geostandards and Geoanalytical Research, 41, 123–135. *Geostandards and Geoanalytical Research*, *43*(2), 317-327. https://doi.org/https://doi.org/10.1111/ggr.12255

Russo, S. C., McCoy-West, A. J., & Duuring, P. (2024). The potential for reconstructing primary ocean chemistry from hypogene and supergene altered banded iron formations: An example from Weld Range, Western Australia. *Precambrian Research*, *413*, 107573. https://doi.org/https://doi.org/10.1016/j.precamres.2024.107573

Sampaio, G. M. S., & Enzweiler, J. (2015). New ICP-MS Results for Trace Elements in Five Iron-Formation Reference Materials [https://doi.org/10.1111/j.1751-908X.2014.00293.x]. *Geostandards and Geoanalytical Research*, *39*(1), 105-119. https://doi.org/https://doi.org/10.1111/j.1751-908X.2014.00293.x

Santrock, J., Studley, S. A., & Hayes, J. M. (1985). Isotopic analyses based on the mass spectra of carbon dioxide. *Analytical Chemistry*, *57*(7), 1444-1448. https://doi.org/10.1021/ac00284a060

Shaheen, M. E., & Fryer, B. J. (2011). A simple solution to expanding available reference materials for Laser Ablation Inductively Coupled Plasma Mass Spectrometry analysis: Applications to sedimentary materials. *Spectrochimica Acta Part B: Atomic Spectroscopy*, *66*(8), 627-636. https://doi.org/https://doi.org/10.1016/j.sab.2011.06.010

Spandler, C., Hammerli, J., Sha, P., Hilbert-Wolf, H., Hu, Y., Roberts, E., & Schmitz, M. (2016). MKED1: A new titanite standard for in situ analysis of Sm–Nd isotopes and U–Pb geochronology. *Chemical Geology*, *425*, 110-126. https://doi.org/https://doi.org/10.1016/j.chemgeo.2016.01.002

Strelow, F. W. E. (1960). An Ion Exchange Selectivity Scale of Cations Based on Equilibrium Distribution Coefficients. *Analytical Chemistry*, *32*(9), 1185-1188. https://doi.org/10.1021/ac60165a042

Tanaka, T., Togashi, S., Kamioka, H., Amakawa, H., Kagami, H., Hamamoto, T., Yuhara, M., Orihashi, Y., Yoneda, S., Shimizu, H., Kunimaru, T., Takahashi, K., Yanagi, T., Nakano, T., Fujimaki, H., Shinjo, R., Asahara, Y., Tanimizu, M., & Dragusanu, C. (2000). JNdi-1: a neodymium isotopic reference in consistency with LaJolla neodymium. *Chemical Geology*, *168*(3–4), 279-281. https://doi.org/https://doi.org/10.1016/S0009-2541(00)00198-4

Terashima, S., Ando, A., Okai, T., Kanai, Y., Taniguchi, M., Takizawa, F., & Itoh, S. (1990). Elemental Concentrations in Nine New GSJ Rock Reference Samples "Sedimentary Rock Series". *Geostandards Newsletter*, *14*(1), 1-5. https://doi.org/https://doi.org/10.1111/j.1751-908X.1990.tb00062.x

Thirlwall, M. F. (1991). Long-term reproducibility of multicollector Sr and Nd isotope ratio analysis. *Chemical Geology*, *94*(2), 85-104. https://doi.org/https://doi.org/10.1016/S0009-2541(10)80021-X

Waheed, S., Rahman, A., Siddique, N., & Ahmad, S. (2007). Rare Earth and Other Trace Element Content of NRCC HISS-1 Sandy Marine Sediment Reference Material. *Geostandards and Geoanalytical Research*, *31*(2), 133-141. https://doi.org/https://doi.org/10.1111/j.1751-908X.2007.00845.x

Wasserburg, G. J., Jacobsen, S. B., DePaolo, D. J., McCulloch, M. T., & Wen, T. (1981). Precise determination of SmNd ratios, Sm and Nd isotopic abundances in standard solutions. *Geochimica et Cosmochimica Acta*, *45*(12), 2311-2323. https://doi.org/https://doi.org/10.1016/0016-7037(81)90085-5

Watkins, P. J., & Nolan, J. (1992). Determination of rare-earth elements, yttrium, scandium and hafnium using cation-exchange separation and inductively coupled plasma-atomic emission spectrometry. *Chemical Geology*, *95*(1), 131-139. https://doi.org/https://doi.org/10.1016/0009-2541(92)90050-F

Watson, J. S. (1996). Fast, Simple Method of Powder Pellet Preparation for X-Ray Fluorescence Analysis. *X-Ray Spectrometry*, *25*(4), 173-174. https://doi.org/https://doi.org/10.1002/(SICI)1097-4539(199607)25:4<173::AID-XRS158>3.0.CO;2-Z

Whitworth, A. J., Brand, H. E. A., Wilson, S. A., & Frierdich, A. J. (2020). Iron isotope geochemistry and mineralogy of jarosite in sulfur-rich sediments. *Geochimica et Cosmochimica Acta*, *270*, 282-295. https://doi.org/https://doi.org/10.1016/j.gca.2019.11.029

Williams, H. M., McCammon, C. A., Peslier, A. H., Halliday, A. N., Teutsch, N., Levasseur, S., & Burg, J.-P. (2004). Iron Isotope Fractionation and the Oxygen Fugacity of the Mantle. *Science*, *304*(5677), 1656-1659. https://doi.org/10.1126/science.1095679

Yu, Z., Robinson, P., & McGoldrick, P. (2001). An Evaluation of Methods for the Chemical Decomposition of Geological Materials for Trace Element Determination using ICP-MS.

Geostandards Newsletter, *25*(2-3), 199-217. https://doi.org/https://doi.org/10.1111/j.1751-908X.2001.tb00596.x